

Crystal Structure Refinements of Ge(*tP12*), Physical Properties and Pressure-induced Phase Transformation Ge(*tP12*) \leftrightarrow Ge(*tI4*)

Aron Wosylus^a, Yurii Prots^a, Walter Schnelle^a, Michael Hanfland^b, and Ulrich Schwarz^a

^a Max-Planck-Institut für Chemische Physik fester Stoffe, Nöthnitzer Straße 40, 01187 Dresden, Germany

^b European Synchrotron Radiation Facility, 6 rue Jules Horowitz, 38043 Grenoble CEDEX, France

Reprint requests to Ulrich Schwarz. E-mail: schwarz@cpfs.mpg.de

Z. Naturforsch. **2008**, *63b*, 608–614; received April 4, 2008

Dedicated to Professor Gérard Demazeau on the occasion of his 65th birthday

Single crystals of the modification Ge(*tP12*) are prepared by compressing semiconductor-grade germanium to pressures above 11(1) GPa and heating to temperatures between 1200(100) and 1500(150) K before a stepwise cooling precedes a complete pressure release. The tetragonal crystal structure of Ge(*tP12*) is refined by means of single crystal X-ray diffraction data collected at ambient conditions ($a = 592.81(2)$, $c = 698.03(3)$ pm, space group $P4_32_12$). The atomic arrangement comprising interconnected spiral chains of fourfold symmetry bears a structural similarity to the high-pressure modification S(*tI16*). High-pressure ambient-temperature powder X-ray diffraction measurements reveal a significant anisotropy of the compressibility compatible with the selected crystal structure description. The determined bulk modulus of Ge(*tP12*) amounts to 70(1) GPa which is in good agreement with theoretical calculations and similar to experimental values of other four-coordinated germanium allotropes. Ge(*tP12*) is a diamagnetic semiconductor with $\chi_0 = -3.1(3) \cdot 10^{-7}$ emu g⁻¹ and $\rho_{300\text{ K}} \approx 6 \Omega\text{ m}$ at 300 K. At 10.1(3) GPa, the beginning of the formation of Ge(*tI4*) indicates the onset of a structural transition. The two-phase region extends up to a maximum pressure of 13.0(5) GPa in the direction of increasing pressures. Upon stepwise decompression, the phase Ge(*tP12*) is reformed from Ge(*tI4*) at 9(1) GPa.

Key words: Germanium, High-pressure Modification, Single Crystal, Magnetic Properties, Electrical Resistivity

Introduction

Binary high-pressure phases of silicon and germanium with alkaline-earth and rare-earth metals are intensely investigated in the context of four-bonded networks and potential thermoelectric materials [1–6]. Some products featuring an excess of elemental germanium contain metastable Ge(*tP12*) after high-temperature high-pressure treatment. The modification, also labelled as Ge-III or Ge-st12, was synthesized for the first time by decompression of germanium from 12 GPa to ambient conditions [7]. *In situ* Raman experiments have provided evidence of a formation directly from the β -Sn-type phase [8, 9]. A later report states that the transformation may be achieved by application of much lower pressures, *e. g.*, 2.5 GPa when the duration time is increased to about three weeks [10], but a subsequent *in situ* re-examination could not reproduce these results [11]. The initial crys-

tal structure solution by trial and error is based on powder X-ray diffraction intensities [12].

We report here crystal growth and structure refinement of Ge(*tP12*). The atomic arrangement is discussed with regard to the recently described chain structure of the sulfur modification S(*tI16*) [13]. The presence of one-dimensional building units in Ge(*tP12*) is experimentally evidenced by the anisotropic lattice parameter changes at high pressures.

Experimental Section

Ge(*tP12*) crystals were prepared by treatment of the starting material Ge(*cF8*) (Chempur 99.9999%) at pressures above 11 GPa and at temperatures between 1200(100) and 1500(150) K. This compression was followed by a temperature decrease to 600(50) K within 30 min, holding at this temperature for typically 1 h before cooling to ambient temperature. Afterwards, pressure was completely released within typically 10 h. For force redistribution and pressure

generation a Walker-type multi-anvil module was used [14] to compress octahedra manufactured from MgO with 5% Cr₂O₃ and with edge lengths of 14 or 18 mm. Heating was performed by means of graphite elements with cylindrical shape. As crucible material, hexagonal boron nitride was found to be suitable. Samples were removed easily from the container, evidencing indirectly that no reactions between the crucible and germanium took place. The observed single-crystal formation is assigned to the higher synthesis temperature in comparison to earlier experiments and to the applied temperature ramp of the present study. Powdered samples of the transformation product are dull grey while larger crystalline particles exhibit a shiny silvery lustre. The material is brittle and appears to be stable in air as indicated by powder X-ray diffraction measurements on a sample which was exposed to air at ambient conditions for a time period of about six months. Attempts to induce the transformation into Ge(*tP12*) at lower pressures were not successful. Whether this is due to the reduced shear stress in the employed set-up or the shorter annealing time remains to be investigated.

For single crystal measurements, crystalline pieces of Ge(*tP12*) were isolated from ingots and fixed with two-component glue to glass fibres. Details of the diffractometer measurements are summarized in Table 1. Refinement of the single-crystal X-ray diffraction intensities was done with SHELXL-97 [15] and visualizations of the crystal structures by means of DIAMOND [16].

Sample characterization was performed by powder X-ray diffraction with a Guinier setup (Huber camera G670 with imaging plate detector, CuK_{α1} radiation, $\lambda = 154.056$ pm, $5^\circ \leq 2\theta \leq 100^\circ$). Lattice parameters were obtained by a least-squares refinement of 54 reflections using LaB₆ (NIST, $a = 415.692$ pm) as an internal standard. The calculated metric was used in the final runs of the structure refinement, for calculations of interatomic distances and as a zero-point basis for analyzing the pressure-induced metrical changes.

For powder X-ray diffraction at high pressures, samples were milled into fine grains by manual grinding in an agate mortar. Appropriate amounts of the powders were placed in steel gaskets using a 4:1 methanol/ethanol mixture as pressure-transmitting medium. The diamond anvil cells for generating high pressures had culet sizes of typically 0.4 mm with initial diameters of the gasket holes corresponding to 0.125 mm. Pressures between ambient and 15.3 GPa were determined by the ruby luminescence method [17]. Powder X-ray diffraction measurements were performed at the undulator beamline ID09A of the European Synchrotron Radiation Facility (ESRF, Grenoble). A bent Si(111) monochromator was used to select a radiation of $\lambda = 41.3$ pm from the white beam. During the exposures samples were oscillated by $\pm 3^\circ$ in order to enhance powder statistics. Intensity recording was performed with an imaging plate which was positioned at a distance of approximately 450 mm from

Table 1. Details of the single-crystal X-ray diffraction experiment^a.

Composition	Ge
Symmetry and space group	tetragonal, $P4_32_12$ (no. 96)
Pearson symbol	<i>tP12</i>
Unit cell parameters ^b :	
<i>a</i> , pm	592.81(2)
<i>c</i> , pm	698.03(3)
<i>V</i> , 10 ⁶ pm ³	245.30(2)
Formula units / unit cell, <i>Z</i>	12
Calculated density, g cm ⁻³	5.90
Size of the crystal, μm ³	40 × 50 × 25
Diffractometer	Rigaku AFC 7
Detector	Mercury CCD
Wavelength; λ , pm	MoK _α ; 71.073
Scans (step, deg)	φ (0.6); ω (0.6)
2 θ_{\max} , deg	63.0
Range in <i>h, k, l</i>	$-8 \leq h \leq 8$; $-7 \leq k \leq 8$; $-10 \leq l \leq 10$
Transmission factors T_{\max}/T_{\min}	0.57/0.47
Number of measured reflections	2103
Number of unique reflections	412
<i>R</i> _{int} for averaging	0.036
Number of observed reflections	402
Observation criterion	$I \geq 2\sigma(I)$
Number of refined parameters	15
<i>R1/wR2</i> [$I \geq 2\sigma(I)$]	0.042/0.098
<i>R1/wR2</i> (all data)	0.043/0.099
Residual density (max/min), e · 10 ⁻⁶ pm ⁻³	+2.36/−2.07

^a Further details of the crystal structure investigation can be obtained from Fachinformationszentrum Karlsruhe, D-76344 Eggenstein-Leopoldshafen, Germany, fax:(+49)7247-808-666; e-mail: crysdta@fiz.karlsruhe.de, on quoting the deposition number CSD-419380; ^b from powder-diffraction data with LaB₆ as internal standard.

the sample in order to use the full resolution of the instrument. For calibration of wavelength and the distance between detector and sample we used a standard silicon sample, Si(*cF8*). Integration of the two-dimensional X-ray diffraction intensities was performed with the FIT2D software [18]. Before refining the intensity data, background caused by Compton scattering of the diamonds was subtracted. X-Ray diffraction profiles were simulated using a modified Lorentz function as implemented in the program package FULLPROF [19]. In order to reduce the number of parameters to be refined, the atomic displacement was described in an isotropic approximation with U_{iso} fixed to 64 pm² ($B_{\text{iso}} = 0.5 \text{ \AA}^2$) for all atoms. In the region in which Ge(*tP12*) and Ge(*tI4*) were coexisting, structural parameters remained fixed and only lattice parameters were refined. The powders of β -tin-type Ge(*tI4*) showed strong preferred orientation along the [001] direction. In the intensity calculations, the effect of texture was accounted for by using a *March-Dollase* function. Atom positions and lattice parameters as resulting from refinements using powder X-ray diffraction data are summarized in Table 2.

Table 2. Refined lattice parameters and atomic positions of the germanium allotropes Ge(*tP12*) and Ge(*tI4*) at elevated pressures. The e. s. d.'s of the determined positional parameters of Ge(*tP12*) are typically 0.001–0.002 and for the pressure approximately 0.1 GPa. In Ge(*tP12*), Ge1 is located on *4a* ($x, x, 0$) and Ge2 on *8b* (x, y, z). In Ge(*tI4*), atoms occupy the position *4a* (0, 0, 0) (origin choice 1).

<i>p</i> (GPa)	Modification	<i>a</i> (pm)	<i>c</i> (pm)	<i>V</i> (10 ⁶ pm ³)	Ge1		— Ge2 —	
					<i>x</i>	<i>x</i>	<i>y</i>	<i>z</i>
0.7	Ge(<i>tP12</i>)	591.64(1)	695.55(1)	245.30(1)	0.090	0.175	0.369	0.258
1.5	Ge(<i>tP12</i>)	589.66(1)	691.16(1)	243.47(1)	0.090	0.175	0.369	0.259
2.4	Ge(<i>tP12</i>)	587.54(1)	686.83(1)	240.32(1)	0.092	0.175	0.369	0.262
3.8	Ge(<i>tP12</i>)	584.83(1)	681.36(1)	237.10(1)	0.092	0.175	0.370	0.263
4.9	Ge(<i>tP12</i>)	583.01(1)	677.68(1)	233.04(1)	0.091	0.172	0.371	0.264
5.7	Ge(<i>tP12</i>)	581.34(1)	674.35(1)	230.34(1)	0.092	0.172	0.372	0.266
7.2	Ge(<i>tP12</i>)	578.85(1)	669.65(1)	227.90(1)	0.094	0.173	0.372	0.269
8.1	Ge(<i>tP12</i>)	577.41(1)	666.94(1)	224.38(1)	0.093	0.174	0.370	0.269
9.3	Ge(<i>tP12</i>)	575.42(1)	663.36(1)	222.36(1)	0.092	0.175	0.366	0.271
9.8	Ge(<i>tP12</i>)	574.84(1)	662.27(1)	219.64(1)	0.093	0.173	0.368	0.273
10.1	Ge(<i>tP12</i>)	573.97(1)	660.79(2)	218.84(1)	0.096	0.174	0.373	0.273
	Ge(<i>tI4</i>)	496(1)	273.2(6)	66.9(1)				
10.3	Ge(<i>tP12</i>)	573.2(1)	659.56(3)	217.69(1)	0.094	0.175	0.370	0.272
	Ge(<i>tI4</i>)	494.45(2)	272.82(3)	66.70(2)				
10.9	Ge(<i>tP12</i>)	572.12(2)	657.76(3)	216.70(1)	0.094	0.178	0.371	0.271
	Ge(<i>tI4</i>)	493.62(1)	272.41(1)	66.38(1)				
11.7	Ge(<i>tP12</i>)	571.26(2)	656.38(4)	215.30(1)				
	Ge(<i>tI4</i>)	492.85(1)	271.87(1)	66.04(1)				
12.1	Ge(<i>tP12</i>)	570.56(3)	655.44(7)	214.20(2)				
	Ge(<i>tI4</i>)	492.29(1)	271.49(1)	65.80(1)				
12.6	Ge(<i>tP12</i>)	570.01(5)	654.4(1)	213.37(3)				
	Ge(<i>tI4</i>)	491.82(1)	271.16(1)	65.59(1)				
13.4	Ge(<i>tP12</i>)	569.00(5)	654.0(2)	212.62(5)				
	Ge(<i>tI4</i>)	490.92(1)	270.55(1)	65.20(1)				
14.1	Ge(<i>tI4</i>)	489.68(1)	269.67(1)	64.66(1)				
15.3	Ge(<i>tI4</i>)	488.94(1)	269.22(1)	64.36(1)				

Table 3. Atomic coordinates and displacement parameters of Ge(*tP12*) at ambient conditions refined using single-crystal X-ray diffraction data^a.

Atom	Site	<i>x</i>	<i>y</i>	<i>z</i>	<i>U</i> _{eq}
Ge1	<i>4a</i>	0.0880(1)	<i>x</i>	0	118(2)
Ge2	<i>8b</i>	0.1715(1)	0.3714(1)	0.25285(9)	120(2)

Atom	Site	<i>U</i> ₁₁	<i>U</i> ₂₂	<i>U</i> ₃₃	<i>U</i> ₁₂	<i>U</i> ₁₃	<i>U</i> ₂₃
Ge1	<i>4a</i>	108(3)	<i>U</i> ₁₁	139(4)	−4(3)	14(3)	−15(3)
Ge2	<i>8b</i>	108(3)	118(3)	135(3)	−9(2)	11(3)	5(4)

^a The *U*_{eq} values (in 10² pm²) are defined as one third of the trace of the *U*_{ij} tensor, the total displacement is defined as $\exp\{-2\pi^2[U_{11}h^2a^{*2} + \dots + 2U_{23}klb^*c^*]\}$.

Magnetization at external fields between 20 Oe and 70 kOe in the temperature range from 1.8 to 400 K was measured in a SQUID magnetometer (MPMS XL-7, Quantum Design) on a polycrystalline sample (mass *m* = 87 mg). The electrical resistivity was determined by a dc four-point method in the range between 4 and 320 K. Due to the uncertainty of the geometry of the electrical connection to the sample and the non-ohmic character of the contacts the inaccuracy of the absolute resistivity is estimated to be up to 50 %, especially at the highest resistances at low temperatures.

Table 4. Interatomic distances (pm) and angles (deg) in Ge(*tP12*) at ambient conditions (single-crystal structure refinement). Bond lengths of the first crystal-structure determination [12] correspond to 248(4), 249(4), and 249(5) pm, respectively.

Ge1–Ge2 (2×)	248.07(8)	Ge1–Ge2 (2×)	248.63(7)
Ge2–Ge1 (1×)	248.07(8)	Ge2–Ge1 (1×)	248.63(7)
Ge2–Ge2 (2×)	250.53(6)		
Ge1–Ge2–Ge2	101.15(5)	Ge1–Ge2–Ge2 (2×)	97.95(2)
Ge1–Ge2–Ge2 (2×)	130.34(3)	Ge1–Ge2–Ge2	103.58(4)
Ge2–Ge1–Ge1	104.96(3)	Ge2–Ge1–Ge2	91.51(3)
Ge2–Ge1–Ge2	136.25(2)	Ge2–Ge1–Ge2	88.00(2)
Ge2–Ge1–Ge2	106.53(3)	Ge2–Ge2–Ge2	119.02(2)

Results and Discussion

In the crystal structure of Ge(*tP12*), germanium atoms are located on two crystallographically different sites of the chiral space group *P4₃2₁2*: the general position *8b* (Ge2) and the special site *4a* (Ge1). At ambient conditions, the refined atomic positions (Table 3) are in good agreement with the earlier values estimated from X-ray powder diffraction data [12]. However, the bond lengths calculated in the present study

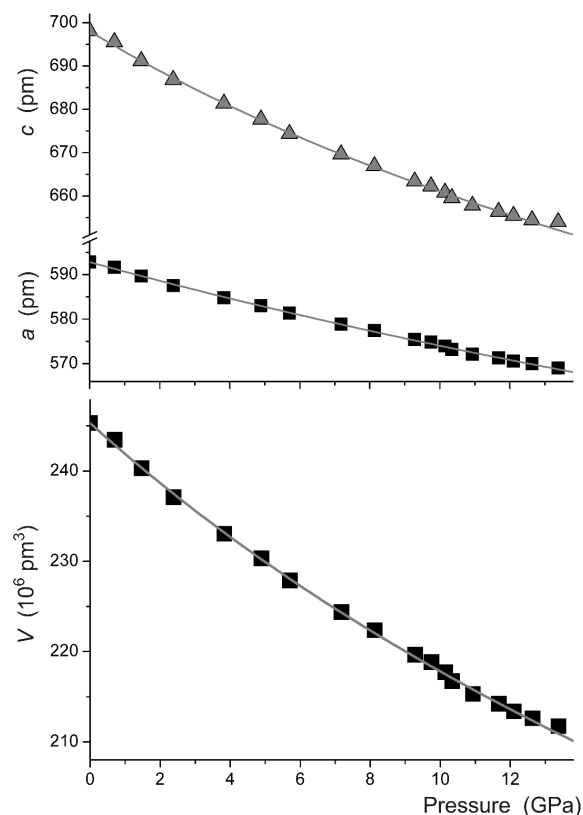


Fig. 1. Lattice parameters a , c and unit cell volume V of Ge(*tP12*) at high pressures. The lines correspond to least-squares fits of Murnaghan-type equations of state to the experimental data.

(Table 4) bear a significantly improved precision due to applying positional parameters refined by means of single-crystal X-ray diffraction intensities with lattice parameters determined from X-ray powder diffraction using an internal standard. As a consequence of the selected procedure, and in contrast to the first determination, the elongation of interatomic distances ranging from 248.07(8) to 250.53(6) pm is significant with respect to diamond-type Ge(*cF8*) adopting a $d(\text{Ge}-\text{Ge})$ of 245 pm at ambient conditions [20]. The refined values for the bond angles fully confirm the marked deviation of the four-coordinated germanium atoms from tetrahedral symmetry. However, the absolute structure resulting from the refinement is considered too poor to warrant publication since the Flack parameter is unstable [21].

In accordance with the first structure solution, the spatial organization of the crystal structure can be depicted as comprising spiral chains of Ge2 atoms ar-

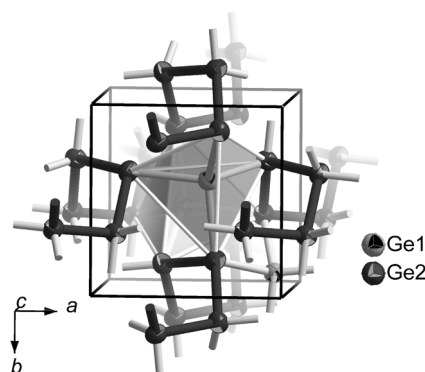


Fig. 2. Crystal structure of Ge(*tP12*). The spiral chains of Ge2 are shown in dark. The coordination polyhedra of the interconnecting Ge1 atoms are indicated by shaded faces. Thick lines connecting spheres represent Ge–Ge bonds.

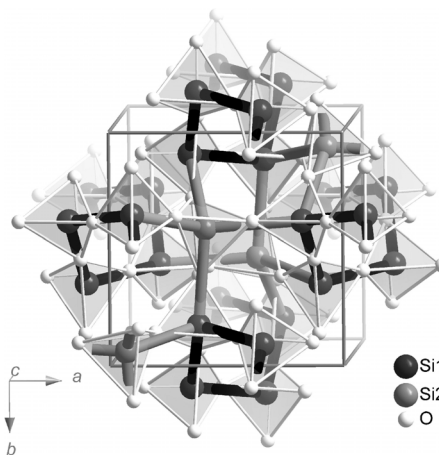


Fig. 3. Crystal structure of SiO₂ in the modification Keatite [22]. The similarity to the crystal structure of Ge(*tP12*) is emphasized by marking the fourfold chains in black, and indicating the interconnecting tetrahedra by white lines and grey faces.

ranged around the 4_3 screw axis. Four neighboring chains are interconnected to a 3D network by Ge1 atoms (Fig. 2). The pronounced anisotropy of the pressure-induced lattice parameter changes (Table 5 and Fig. 1) is consistent with the presence of low-dimensional building units in the crystal structure. The structure motif has a binary counterpart in the SiO₂ modification Keatite (Fig. 3, [22]) with silicon atoms occupying the germanium positions [12]. However, we note here the structural similarity of Ge(*tP12*) to a recently determined high-pressure chain structure of sulfur, S(*tI16*), adopting space group $I4_1/acd$. This modification of sulfur comprises alternating sequences of chains arranged around 4_1 and 4_3 screw axes, respec-

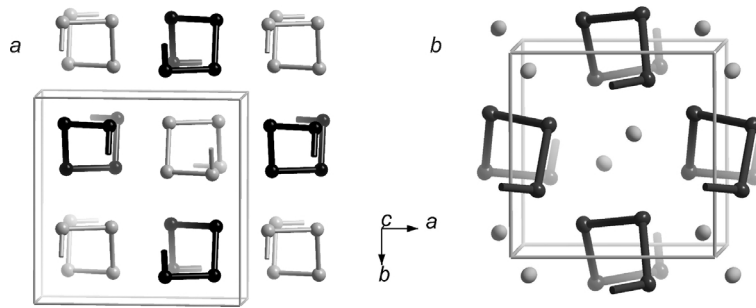


Fig. 4. Crystal structures of the high-pressure modifications of a) *S(tI16)* adopting space group $I4_1/acd$ [13] and b) *Ge(tP12)* with space group $P4_32_12$. Unit cells are indicated by solid lines (for sulfur in the setting origin choice 1). The chains around the 4_3 screw axis are indicated in black, spirals around the 4_1 screw axis in sulfur and interconnecting Ge1 atoms are shown in grey.

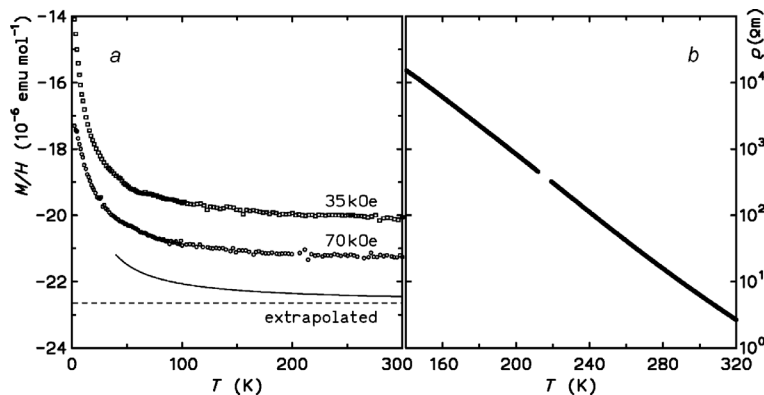


Fig. 5. a) Molar magnetic susceptibility $\chi = M/H$ vs. temperature T of a polycrystalline sample of *Ge(tP12)* in magnetic fields of 70 and 35 kOe (open symbols) and the extrapolated susceptibility of the pure phase (solid line). b) Electrical resistivity ρ of a polycrystalline sample of *Ge(tP12)* versus temperature T .

tively [13]. Despite differences in the spatial arrangement of the spiral chains around the 4_3 screw axis, *Ge(tP12)* can be described as a related defect variety in which the one-dimensional building units formed by Ge2 are linked by Ge1 atoms (Fig. 4). The multiplicity of the Ge1 position amounts to only half of that of the Ge2 site so that the number of atoms in the unit cell is reduced from sixteen in *S(tI16)* to twelve in *Ge(tP12)*.

The high-field magnetic susceptibility $\chi(T) = M/H$ of *Ge(tP12)* is negative (diamagnetic) in the measured temperature range. After taking into account minor para- and ferromagnetic impurities (by a Curie term and by the extrapolation of χ vs. $1/H$ to $1/H = 0$, respectively) a value of $\chi_0 = -3.1(3) \cdot 10^{-7} \text{ emu g}^{-1}$ is calculated (Fig. 5a). In comparison with *Ge(cF8)* ($\chi_0 = -1.06 \cdot 10^{-7} \text{ emu g}^{-1}$ [20]) and *Ge(cF136)* ($\chi_0 = -3.1(2) \cdot 10^{-7} \text{ emu g}^{-1}$ [23]), *Ge(tP12)* is surprisingly strongly diamagnetic. In lower fields no anomalous signals were detected. The resistivity $\rho(T)$ of *Ge(tP12)* is measured in the temperature range 140 to 300 K (Fig. 5b) and shows a thermally activated behavior with a value $\rho_{300 \text{ K}} \approx 6 \Omega \text{ m}$ at 300 K and an estimated lower limit of the energy gap of 0.35 eV (from a fit in the temperature range 285 to 320 K). This estimated value of the energy gap may be reduced with

Table 5. Bulk moduli of lattice parameters a , c and volume V as determined by least-squares fits of Murnaghan-type equations of state [24] to the experimental data.

Parameter	B_0 (GPa)	B'_0
a	273(4)	7.8(9)
c	143(3)	9.0(6)
V	70(1)	3.0(3)

respect to the fundamental band gap due to defects and impurities.

Application of pressures below 10.1(3) GPa induces a continuous compression of *Ge(tP12)* described by $B_0 = 70(1)$ and $B'_0 = 3.0(3)$ GPa when fitting a Murnaghan-type equation of state [24] to the experimental data (Table 5). The fitted bulk modulus B_0 differs significantly from $B_0 = 102(5)$ GPa determined in an earlier investigation [25]. Regarding this pronounced difference, we point out that the homogeneity of the present sample and the accurate measurement of the high-pressure data are evidenced by the result that the extrapolated V_0 of the high-pressure data corresponds within experimental error of the experimentally determined value at ambient conditions. Moreover, the values of $B_0 = 66$ GPa [26] and 73 GPa [27] calculated from quantum mechanical computations are in excellent agreement with the recent experimental result. The

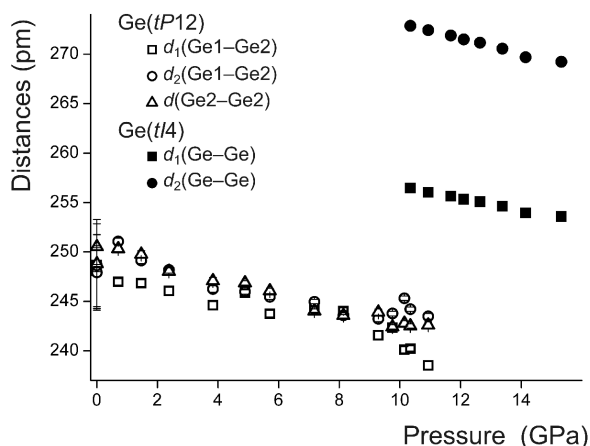


Fig. 6. Interatomic distances in Ge(*tP12*) and Ge(*tI4*) at different pressures. The scattering of data at pressures around 10 GPa is attributed to the solidification of the liquid pressure medium and the onset of the structural phase transition. The error bars of the ambient pressure data refer to literature data [8].

determined quantity is similar to that of other four-bonded germanium modifications like Ge(*cF8*) with $B_0 = 75$ [28], Ge(*cF136*) with $B_0 = 76(6)$ or Ge(*hR8*) with $B_0 = 73(3)$ GPa [29].

The compression leads to a clearly anisotropic change of lattice parameters (see Fig. 1) which reflects the spatial organization of the atoms in the crystal structure. The metrical anisotropy is not immediately visible in the changes of the interatomic distances (Fig. 6) since the orientation of the interatomic bonds has components in both the less and the more compressible directions of the atomic arrangement. The abrupt increase of bond lengths associated with the structural change into the denser modification Ge(*tI4*) is in full agreement with the empirical pressure-distance paradoxon.

At pressures above 10.1(3) GPa, the appearance of new diffraction lines indicates the onset of a structural transformation of Ge(*tP12*) into the β -Sn-type modification Ge(*tI4*). The two-phase region extends up to 13.3(5) GPa. Diffraction patterns of the modifi-

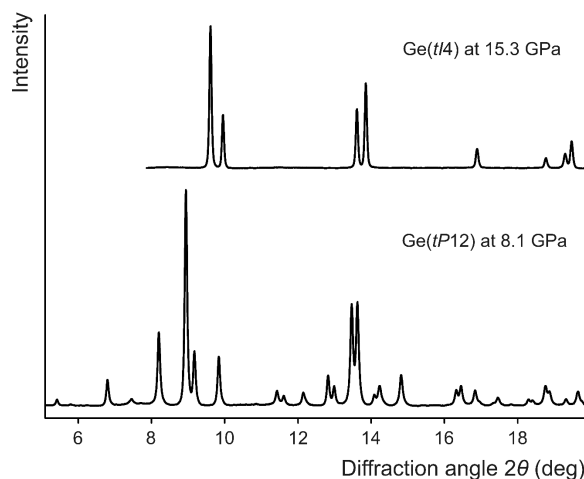


Fig. 7. X-Ray powder diffraction patterns of germanium recorded at elevated pressures in a diamond anvil cell using synchrotron radiation of ID09A of the ESRF ($\lambda = 41.3$ pm).

cations are shown in Fig. 7. Upon stepwise decrease of pressure, the first diffraction lines of Ge(*tP12*) reappear at 9(1) GPa. Further release to pressures between 7 and 5 GPa results in patterns which contain no less than four different germanium modifications: Ge(*tI4*), Ge(*tP12*), Ge(*cF8*) and Ge(*hR8*). The coexistence of the allotropes is compatible with the small energy differences of the germanium modifications as calculated in quantum theoretical computations [30]. In an earlier study, formation of yet another allotrope, Ge(*cI16*), has been reported upon rapid decompression within less than a second [31]. The observation of a large number of competing phases is an impressive direct experimental evidence for the kinetic control of the pressure-induced phase transition of germanium at ambient temperature.

Acknowledgements

We thank Dr. Horst Borrmann and Prof. Yuri Grin for helpful discussions. We like to express our gratitude to Susann Leipe, Carola Müller and Knut Range for supporting high-pressure syntheses. We are grateful to Miriam Schmitt and Katrin Meier for enduring help with the high-pressure X-ray diffraction experiments at ID09A of the ESRF.

- [1] H. Fukuoka, S. Yamanaka, *Phys. Rev. B* **2003**, 67, 094501.
 [2] H. Fukuoka, S. Yamanaka, E. Matsuoka, T. Takabatake, *Inorg. Chem.* **2005**, 44, 1460.
 [3] A. Wosylus, Yu. Prots, U. Burkhardt, W. Schnelle, U. Schwarz, Yu. Grin, *Solid State Sci.* **2006**, 8, 773.

- [4] A. Wosylus, Yu. Prots, U. Burkhardt, W. Schnelle, U. Schwarz, Yu. Grin, *Z. Naturforsch.* **2006**, 61b, 1485.
 [5] S. Yamanaka, S. Maekawa, *Z. Naturforsch.* **2006**, 61b, 1493.
 [6] A. Wosylus, Yu. Prots, U. Burkhardt, W. Schnelle, U. Schwarz, *Sci. Techn. Adv. Mat.* **2007**, 8, 383.

- [7] F. P. Bundy, J. S. Kasper, *Science* **1963**, *139*, 340.
- [8] R. J. Kobliska, S. A. Solin, M. Selders, R. K. Chang, R. Alben, M. F. Thorpe, D. Weaire, *Phys. Rev. Lett.* **1972**, *29*, 725.
- [9] M. Hanfland, K. Syassen, *High Pressure Res.* **1990**, *3*, 242.
- [10] C. H. Bates, F. Datchell, R. Roy, *Science* **1965**, *147*, 860.
- [11] S. B. Quadri, E. F. Skelton, A. W. Webb, *J. Appl. Phys.* **1983**, *54*, 3609.
- [12] J. S. Kasper, S. M. Richards, *Acta Crystallogr.* **1964**, *17*, 752.
- [13] O. Degtyareva, E. Gregoryanz, M. Somayazulu, P. Dera, H. K. Mao, R. J. Hemley, *Nature Mater.* **2005**, *4*, 152.
- [14] D. Walker, M. A. Carpenter, C. M. Hitch, *Am. Mineral.* **1990**, *75*, 1020.
- [15] G. M. Sheldrick, SHELXL-97. Program for the Refinement of Crystal Structures. University of Göttingen, Göttingen (Germany) **1997**.
- [16] K. Brandenburg, DIAMOND (version 3.0c), Crystal and Molecular Structure Visualization, Crystal Impact, Bonn (Germany) **1998**.
- [17] G. J. Piermarini, S. Block, J. D. Barnett, R. A. Forman, *J. Appl. Phys.* **1975**, *46*, 2774; H. K. Mao, P. M. Bell, J. W. Shaner, D. J. Steinberg, *J. Appl. Phys.* **1978**, *49*, 3276.
- [18] A. Hammersley, FIT2D, One- and Two-dimensional Diffraction Data Analysis System, ESRF, Grenoble (France) **1996**. See also: A. P. Hammersley, S. O. Svensson, M. Hanfland, A. N. Fitch, D. Häusermann, *High Pressure Res.* **1996**, *14*, 235.
- [19] J. Rodriguez-Carvajal, *Physica B* **1993**, *192*, 55.
- [20] J. Emsley, *The Elements*, Clarendon press, Oxford **1991**.
- [21] H. D. Flack, G. Bernadelli, *J. Appl. Crystallogr.* **2000**, *33*, 1143.
- [22] J. Shropshire, P. P. Keat, P. A. Vaughan, *Z. Kristallogr.* **1959**, *112*, 409.
- [23] A. Guloy, R. Ramlau, Z. Tang, W. Schnelle, M. Baitinger, Yu. Grin, *Nature* **2006**, *443*, 320.
- [24] F. D. Murnaghan, *Proc. Natl. Acad. Sci. U.S.A.* **1944**, *30*, 244.
- [25] C. S. Menoni, J. Z. Hu, I. L. Spain, *Phys. Rev. B* **1986**, *34*, 362.
- [26] A. Mujica, R. Needs, *Phys. Rev. B* **1993**, *48*, 17010.
- [27] J. Crain, S. J. Clark, G. J. Ackland, M. C. Payne, V. Milman, P. D. Hatton, B. J. Reid, *Phys. Rev. B* **1994**, *49*, 5329.
- [28] M. W. Guinan, D. J. Steinberg, *J. Phys. Chem. Solids* **1974**, *35*, 1501; K. A. Gschneidner, *Solid State Phys.* **1964**, *16*, 275.
- [29] U. Schwarz, A. Wosylus, B. Böhme, M. Baitinger, M. Hanfland, Yu. Grin, unpublished results.
- [30] A. Mujica, S. Radescu, A. Munoz, R. J. Needs, *High Pressure Res.* **2001**, *22*, 455.
- [31] R. J. Nelmes, M. I. McMahon, N. G. Wright, D. R. Allan, J. S. Loveday, *Phys. Rev. B* **1993**, *48*, 9883.